

Thermoreversible Gels of Polyaniline: Viscoelastic and Electrical Evidence on Fusible Network Structures

Terhi Vikki, Janne Ruokolainen, and Olli T. Ikkala*

Department of Engineering Physics and Mathematics, Helsinki University of Technology, P.O. Box 2200, FIN-02015 HUT Espoo, Finland

Pentti Passiniemi

Neste Oy, Corporate Technology, P.O. Box 310, FIN-06101 Porvoo, Finland

Heikki Isotalo

VTT Electronics, Electronic Materials and Components, Technical Research Centre of Finland, P.O. Box 1101, FIN-02044 VTT Espoo, Finland

Mika Torkkeli and Ritva Serimaa

Department of Physics, University of Helsinki, P.O. Box 9, FIN-00014 Helsinki, Finland

Received October 10, 1996; Revised Manuscript Received April 9, 1997^o

ABSTRACT: We demonstrate *thermoreversible* gelation of a conductive polymer, i.e., rubber-like melt processible electrically conducting compounds. Combination of viscoelastic and electrical conductivity measurements suggests network formation in the gel state and gel melting at elevated temperatures. The gels have been prepared by dissolving polyaniline in dodecylbenzenesulfonic acid (DBSA) using formic acid as a processing medium which was removed at the end. Importantly, without formic acid, reversible gelation and particle-free materials were not achieved even at the resolution of optical microscopy. For $T < T_{\text{gel}}$ the materials behave elastically in compression experiments, the storage and loss moduli do not depend much on frequency, and the electrical conductivity is primarily *electronic*, probably due to high chain-to-chain hopping conductivity. For $T > T_{\text{gel}}$ the onset of liquid-like flow is detected using modified ball drop method by dynamic mechanical analysis, the dynamic moduli become strongly frequency dependent, and the electrical conductivity drops orders of magnitude to the value corresponding to the ionic conductivity of DBSA, suggesting that the chains are not in direct contact. The physical cross-links are probably localized mesomorphic domains which allow melting.

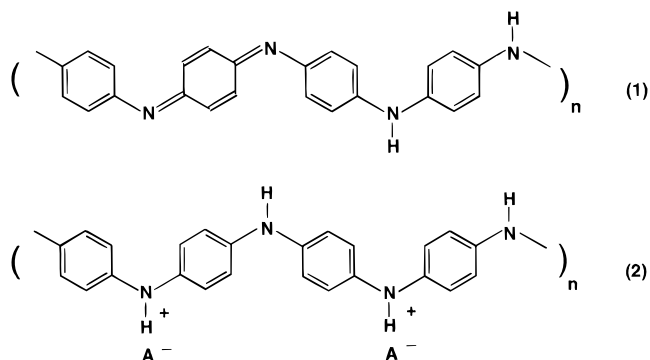
Introduction

Reversible gelation in polymer–solvent systems has been extensively studied during the recent years due to its interesting connections with polymer–solvent phase behavior, network formation, and aggregation.^{1–5} Thermoreversible gels differ from the chemical gels in that the cross-links, being only of physical origin, can be reversibly purged and reformed by adjusting the temperature. Different types of physical cross-links have been reported, such as micellar crystallites, side chain crystallinity in comb-shaped polymers, and triple helices or glassy aggregates.^{6,7} Definition of gels may vary from author to author.³ However, a system defined as a gel contains a network, leading to elastic behavior.⁴ Reversible gelation has been reported for many systems consisting of flexible polymers, e.g., *i*-polystyrene/*cis*-decalin, *α*-polystyrene/carbon disulfide, and gelatin/water.^{1,3,4} Proper complexation with solvent molecules opposes chain folding to lamellae, thus promoting aggregation in the extended conformation.⁴

Gelation of more rigid rod polymers has been studied by cooling their solutions or adding nonsolvents.^{1,3} An example which is relevant to the present work is poly-(1,4-phenylene-2,6-benzobisthiazole) (PBT) in combination with methanesulfonic acid (MSA).⁸ MSA is a solvent which also protonates PBT. Coagulation in aqueous solution or absorption of atmospheric humidity yields network structure.^{9,10} Gelling has also been studied for poly(γ -benzyl glutamate) (PBLG) using

dimethylformamide (DMF) as a solvent and water as a nonsolvent¹¹ and also in benzyl alcohol (see a recent article¹²).

Electrically conductive polymers are rigid or semirigid polymers.¹³ At present, the most feasible candidate for bulk applications is polyaniline (PANI); see eq 1 for the insulating emeraldine base (EB) form:^{14,15}



The EB form can be doped by strong acids (A^-H^+)¹⁶ to form the electrically conductive emeraldine salt (ES) form; see eq 2 (for an early example, see ref 17). ES is regarded as “intractable”, i.e., it does not melt before decomposition. Emeraldine salts are soluble in strong acids, as demonstrated by high solubility of emeraldine hydrochloride in H_2SO_4 .¹⁸ Also excess amounts of dodecylbenzenesulfonic acid (DBSA) both dope and plasticize EB.^{19–21} Identification of less acidic solvents and plasticizers for ES was long regarded difficult. However, PANI doped by camphorsulfonic acid (CSA)

* Corresponding author.

^o Abstract published in *Advance ACS Abstracts*, June 1, 1997.

was observed to be highly soluble in phenols¹⁹ as explained by molecular recognition effects.²² Also plasticizers (a special case of solvents) for ES have been found, such as compounds capable of coordination complexation,²³ and compounds capable of sterically tailored hydrogen bondings and phenyl stacking (i.e., a form of molecular recognition).^{22,24,25}

Gels have been discussed primarily in two contexts in electrically conducting polymers. Firstly, it is known that sufficiently concentrated PANI solutions tend to undergo gelation with time.^{26,27} A nonprocessible physical gel is easily formed (unless special tricks are performed to dope and undope the material several times²⁶). The physical cross-link sites are probably crystallites which may need very high temperatures to melt. As another example, in their efforts to understand conformations and to achieve true molecular solution of PANI doped by CSA in *m*-cresol, Gettinger et al. in some cases observed gelation, especially if water was present.²⁸ Work to reduce aggregation in PANI solutions by incorporating LiCl has been reported²⁹ and improved solution stability has been achieved by proper selection of solvents.³⁰ Secondly, the swelling properties of poly(3-alkylthiophenes) that have been chemically cross-linked are also studied.^{31–33}

In our present work, we took a novel point of view and asked the following questions: (1) Can one construct PANI gels that melt, i.e., can be processed at elevated temperatures? (2) What are the viscoelastic and electrical properties and the phase behavior of such potential *thermoreversible* gels? If possible, a reversible PANI *network* is then expected with an elastic "rubber-like" behavior and high electrical conductivity in the gel state. In the solution state, one expects dissolution of PANI chains in the solvent, i.e., disruption of the networks, with the expected liquid-like flow and reduction or even loss of electrical conductivity.

The above questions address both the viscoelastic and electrical aspects of the formation of percolative networks. Network formation in conductive polymers has been studied,^{34–36} and networks are shown to be ultimately dispersions in some cases.^{37–39} Note that the observed network in PANI(CSA)/polymethyl methacrylate³⁴ was prepared by solution casting. Therefore, a heating would probably lead to disruption of the network and suggests that the network is not fusible. In addition, the role of percolation in the context of gel formation has also been amply discussed (see the book by Cohen Addad⁴⁰).

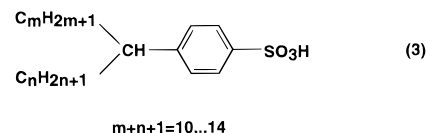
In selecting a suitable system, we chose DBSA as the solvent because we expected it to hinder the potentially irreversible crystallite formation of PANI due to its size. The literature of rigid rod polymers suggested to investigate suitable nonsolvents for PANI/DBSA to act as coagulants, such as water, different carboxylic acids, and hydroxyl-containing compounds. We screened a large number of such potential candidates and were, so far, able to identify only one, i.e., formic acid (HCOOH), which clearly rendered thermoreversible gels. It turned out unique also in another respect: If PANI/DBSA complexes are prepared in formic acid (and later removed), particle-free films at the resolution of an optical microscope were achieved. Omission of formic acid or use of another medium rendered clear dispersions.

Experimental Section

Materials. EB form of PANI was polymerized at Neste Oy (Finland) by using conventional methods.⁴¹ The viscosity was

0.88 dL/g measured by an Ubbelohde viscometer for a 0.1 wt % solution in 97 wt % sulfuric acid at 25 °C. The molecular weights are $M_n = 25\,000$ and $M_w = 120\,000$ determined by GPC. It was calibrated with commercial PS standards using *N*-methylpyrrolidone/0.2 M LiCl eluent at room temperature. PANI was dried at 60 °C in vacuum for 2 days and subsequently stored in a desiccator.

DBSA was of laboratory purity (Tokyo Kasei) and used without further purification. The structure according to the manufacturer is shown in eq 3 where the dominant length of



the alkyl chain ($m + n + 1$) is 12. Sulfonic acids are very hygroscopic, as was pointed out early by Vold.⁴² The water content of the present DBSA is low, i.e., 0.01–0.7% according to the manufacturer. In order to avoid absorption of additional humidity, DBSA was stored and opened only in a dry nitrogen atmosphere. Formic acid (99%) was supplied by Riedel & Haen and used as such.

Sample Preparation. Samples with five weight ratios of the EB form of PANI and DBSA were prepared, i.e., 21.7/78.3, 15.6/84.4, 12.2/87.8, 10.0/90.0, and 7.3/92.7 (w/w). They were prepared in formic acid in the following way. PANI and DBSA at their total weight fraction of 2.5 wt % were mixed with 97.5 wt % formic acid and stirred at 60–80 °C for 24 h using a magnetic stirrer. Subsequently, the formic acid was evaporated on a hot plate at 80 °C, and the mixtures were dried in vacuum at 60 °C for 1 week. Samples were stored in a desiccator. FTIR and mass spectrometry (heating up to 380 °C in vacuum) did not show signs of residual formic acid. Importantly, at the resolution of optical microscopy a homogeneous particle-free morphology was obtained without a need for centrifugation.

We also point out that initially a considerable effort was made to prepare completely anhydrous samples making all operations in a glovebox under N_2 gas using distilled reagents. It turned out, however, that formic acid is somewhat unstable with formation of CO and H_2O in the present process. Therefore, slight amounts of humidity cannot easily be avoided during the dissolution stage in formic acid, and the simpler scheme of sample preparation as described above was used.

General Comments on Characterization. Note that the strongly acidic nature of the present samples prohibited the conventional characterization using differential scanning calorimetry and dynamic rheometer.

Compression/Relaxation Experiments. Experiments with cyclic compression and relaxation were performed under helium gas using a Perkin-Elmer DMA 7 apparatus to study whether rubber-like behavior was achieved. The measurement is a modification of the method used by Guenet et al.⁴ Cylindrical samples with a diameter of ca. 4 mm and a height of ca. 2 mm were cut. The sample was first compressed to 80% of the original thickness for 30 min, i.e., $\lambda = L/L_0 = 0.8$, where L = the deformed thickness and L_0 = the initial thickness. Thereafter, the compression was removed, and the relaxation of the sample thickness L was measured as a function of time for 120 min. The cycle was repeated.

Mechanical Characterization of Gel Melting by Modified Ball Drop Method. The simplest method to determine the gel melting is the sc ball drop method (BDM) where a steel ball starts to penetrate the material during slow heating when melting takes place.⁴³ Here we adopted its modification: A cylindrical sample (thickness 2–4 mm and diameter ca. 5 mm) was placed between two parallel plates in a dynamic mechanical analyzer (Perkin Elmer DMA 7). The top plate vibrated at a frequency of 1 Hz using a small net compressive stress. The sample was heated at the rate 3 °C/min, and gel melting was observed at the temperature where the top plate started to penetrate the sample due to onset of flow (see the inset of Figure 3). The measurements were performed under helium gas.

Rheological Characterization of Gel Melting. We again used a variation of BDM using a Perkin Elmer DMA 7 instrument. The dynamic mechanical storage and loss moduli E' and E'' of cylindrical samples were measured isothermally as a function of frequency using a vibrating parallel plate mode. The temperatures were 20, 60, 100, 160, 180, and 200 °C, and the frequency range was from 0.01 to 30 Hz. Because the method is applicable for solid materials which do not flow substantially, only the onset of the melting transitions could be detected reliably as the temperature was increased. The samples were under helium gas.

Room Temperature Conductivity. At room temperature, the conductivities were measured using the conventional four-probe technique with pressed contacts. The sample dimensions were ca. $3 \times 1 \times 1$ mm³. Five constant current values were imposed for ca. 10 s each, ranging from negative to positive values (see the inset of Figure 5), and the corresponding voltage was averaged for each current. The resistance and thus the conductivity were determined from the linear current–voltage behavior. Therefore, the measurement can be regarded as a low-frequency AC measurement using a triangular waveshape at the frequency of ca. 20 mHz. The measurements were done under atmospheric conditions shortly after taking the samples out of the desiccator.

Conductivity as a Function of Temperature. As a function of temperature, the resistances were measured using a Linkam TMS 91 hot stage in combination with a four-probe system. At each temperature, five constant current values were imposed, as in the previous section. However, higher frequency was used for the imposed triangular waveshape of the current, i.e., ca. 200 mHz. The currents were less than 10 μ A. The samples were pressed on a glass plate containing four Au electrodes whose relative distance was ca. 0.2 mm. The typical thickness of the sample was 0.1 mm and width 1–2 mm. The heating rates of 5, 25, and 75 °C/min were used. The samples were under N₂ gas. The temperature was measured with a thin thermocouple thermally attached on top of the glass plate. Two cooling procedures were used: either at the same rate as the heating or by quenching to room temperature during a few seconds. The resistances of the samples were measured. For selected samples, several heating/cooling cycles were performed and the behavior during repeated cycles was observed to be similar to that in the first cycle. Additionally, for selected samples AC conductivity measurements at 5, 500, and 1000 Hz showed essentially similar results (comprehensive results will be published separately).

Small Angle X-ray Scattering. The Cu K α radiation was monochromatized by means of the combined action of a Ni filter and a totally reflecting mirror (Huber small angle chamber 701). The sealed Cu anode fine focus X-ray tube was powered by a Siemens Kristalloflex 710 H. The scattered radiation was detected by a linear one-dimensional position sensitive proportional counter (MBraun OED-50M). The X-ray tube was mounted in the point-focusing position, and the beam and the detector heights were sufficiently reduced so that there were no significant smearing effects in the diffraction peaks due to instrumental broadening. However, the samples being weak scatterers, the instrumental function in the vertical direction was allowed to have fwhm up to 0.1 Å⁻¹. The beam was still narrow, fwhm < 0.002 Å⁻¹. The smallest achievable k is only ca. 0.02 Å⁻¹ using this setup. The results have been plotted by using the magnitude of the scattering vector $k = (4\pi/\lambda) \sin \theta$, where $\lambda = 1.542$ Å and 2θ is the scattering angle. Background scattering was subtracted from the experimental intensity curve.

Wide Angle X-ray Scattering. The samples were pressed pellets with a thickness of 1 mm and a diameter of 20 mm. The temperature was 25 °C, and a two-circle diffractometer was used in the symmetrical transmission mode. The measurements were made with Mo K α ($\lambda = 0.709$ Å) radiation monochromatized with a diffracted beam monochromator (LiF (200)). The intensity curves were measured with a scintillation counter. The air scattering was subtracted. The magnitude of the scattering vector k was calculated as in SAXS measurements.

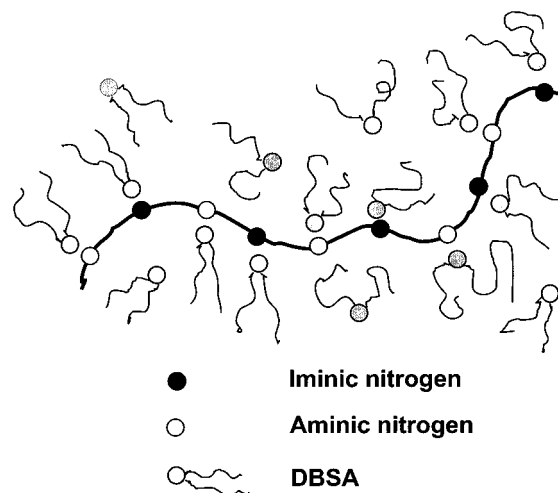


Figure 1. Scheme of the complexation of a PANI (EB) chain with DBSA molecules.

UV/Vis Measurements. UV/vis spectra were measured using a Hitachi U-2000 spectrophotometer and a Linkam TMS 91 hot stage at room temperature and at 150 °C. The spectra ranged from 200 to 1100 nm. The samples were between two glass plates during the measurements. The part from 200 to about 350 nm contained absorption from the glass and is therefore omitted.

Results

Figure 1 shows a schematic picture of the expected architecture of a PANI chain dissolved in DBSA. The iminic nitrogens are protonated by DBSA, and the aminic sites are probably hydrogen bonded to DBSA. Therefore, a comb-shaped chain is expected, here denoted as PANI(DBSA)_{1.0}. Additional DBSA is in the background medium, not bonded to PANI. Therefore, in the present work it is studied whether PANI(DBSA)_{1.0} forms a reversible network in the DBSA medium. The network would affect elastic properties and electrical conductivity. Gel melting would result if the physical cross-links of the network can be reversibly purged at high temperatures, due to dissolution. Because the conductivity can be decomposed into *intrachain conductivity* along the chains and *interchain hopping* between the chains, it can be expected that dissolution and networking would yield also different conduction behavior. The interchain conductivity is expected to be the limiting factor for the total conductivity. For dissolved chains, the hopping conductivity is expected to be low, and the total conductivity would be determined by the ionic conductivity of the DBSA medium between the chains. For networks, higher conductivity due to the direct chain-to-chain hopping conductivity would be expected, potentially not showing ionic conductivity.

Based on the validity of the above hypothesis, gel melting is expected to manifest in onset of flow, in dynamic storage and loss moduli as functions of frequency, in ionic vs electronic conductivity vs PANI weight fraction, and in conductivity vs temperature. Experimental results will be presented along these lines.

Elastic behavior is studied using compression/relaxation measurements. Figure 2 shows how the sample thickness $L(t)$ recovers following a compression to 80% of the original thickness L_0 for three PANI/DBSA samples. Samples with 15.6 or 10.0 wt % PANI show almost complete recovery of the thickness in the repeated compressions, as is illustrated between cycles 1 and 2. In contrast, after the first compression, the

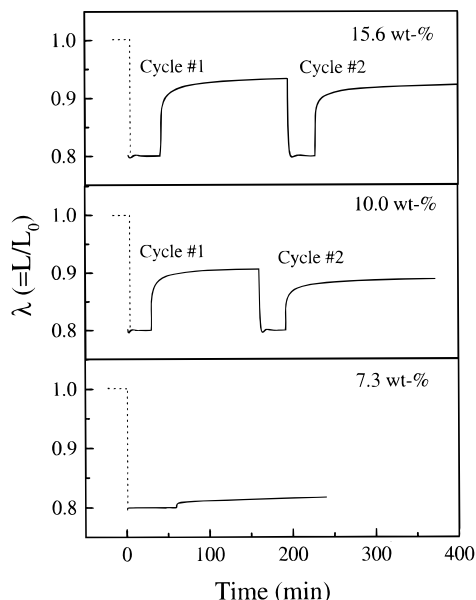


Figure 2. Scaled thickness $\lambda = L/L_0$ of PANI/DBSA with three weight fractions of PANI as a function of time during compression testing. L = thickness of the sample, and L_0 = original thickness. At time $t = 0$ the sample is compressed to 80% of the original thickness, i.e., $\lambda = 0.8$, and the recovery of the dimensions is followed after the compression is relieved.

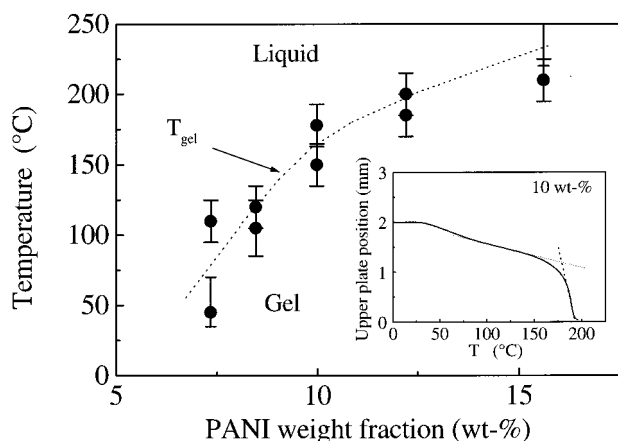


Figure 3. Gel melting temperatures T_{gel} of PANI/DBSA as a function of PANI weight fraction, as determined by the onset of flow using DMA parallel plate mode at sweep rate 3 °C/min and 1 Hz (modified ball drop method).

original thickness is not completely recovered probably due to sample imperfections, such as voids and inaccuracies in cutting the sample phases exactly parallel. The observed elastic behavior in repeated cycles strongly suggests networking, in analogy with cross-linked rubber. Reduced amount of PANI (i.e., 7.3 wt %) yields almost no elastic recovery, suggesting incomplete network. Note, however, that the sample still does not flow at room temperature. Therefore it can be regarded as "a limiting case gel", still fulfilling the condition of "no steady state flow".³

Onset of flow indicating gel melting is observed at elevated temperatures using dynamic mechanical analysis. As an example, the inset of Figure 3 shows the position of a plate vibrating at 1 Hz against the sample surface as a function of the temperature (modified BDM method). Onset of flow is observed for the given sample PANI/DBSA 10/90 (w/w) at a $T_{gel} = \text{ca. } 180^\circ\text{C}$. For selected samples the measurement was repeated and in the second heating the melting took place essentially

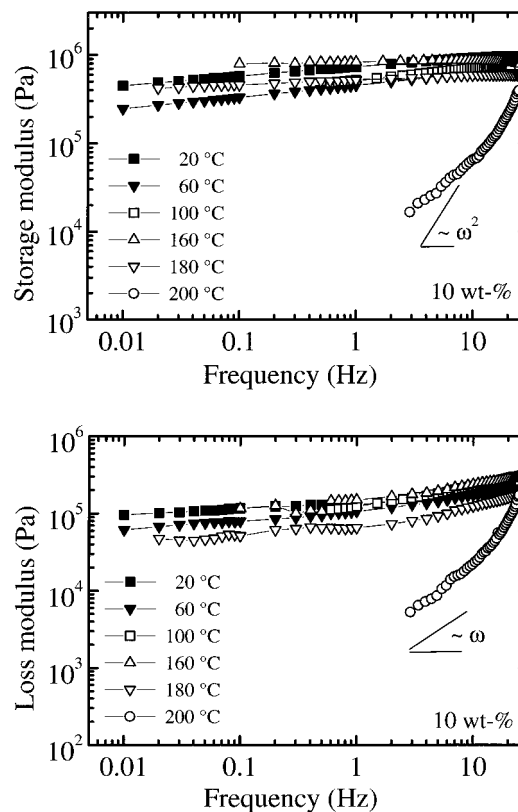


Figure 4. (a) E' and E'' (b) for PANI/DBSA with 10.0 wt % PANI as a function of frequency in the parallel plate mode of DMA at the fixed temperatures of 20, 60, 100, 160, 180, and 200 °C.

at the same temperature as in the first heating. Figure 3 shows that lower T_{gel} is observed for lower PANI concentrations. The decrease of PANI weight fraction to less than ca. 7 wt % rendered viscous fluids instead of elastic gels. The sample containing 21.7 wt % of PANI (or more) remained as an infusible powder at all temperatures studied.

The gels are expected to show moduli that are essentially independent of frequency at low ω .³ Dynamic mechanical measurements as a function of frequency were performed in the parallel plate mode for PANI/DBSA 10/90 (w/w) at several temperatures (see Figure 4). At 20, 60, 100, 160, and even 180 °C, the storage and loss moduli (E' and E'') are relatively constant as a function of the available frequency and essentially do not depend on the temperature, in agreement with the solid-like behavior of gels.⁶ A drastic change is observed as the temperature is increased from 180 to 200 °C where a strongly frequency dependent behavior is observed. Homopolymer melts would give $E' \sim \omega^2$ and $E'' \sim \omega$. Note that the present data at 200 °C are not far from such behavior, although measurements in the liquid state performed using the parallel plate setup should be taken with some precaution. Above 200 °C the measurement could not be reliably made using DMA, because of the high fluidity of the samples.

The DMA results as a function of frequency and temperature can be discussed in the perspective of physical gelling studies on poly(vinyl chloride)/dioctyl phthalate (i.e., PVC/DOP), as reviewed by, for example, te Nijenhuis,⁶ 10 wt % PVC dissolves in 90 wt % DOP at the elevated temperature (ca. 160 °C). Shortly after quenching to 90 °C, which is below the gelation temperature, a strongly frequency dependent storage modu-

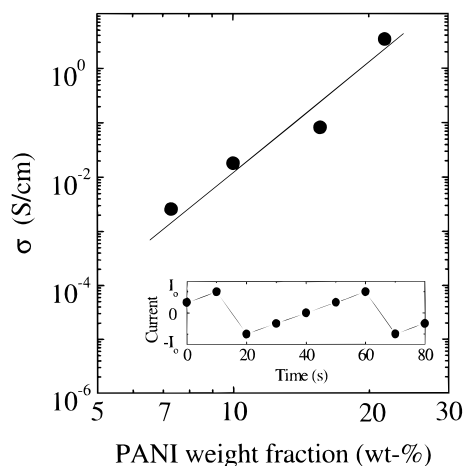


Figure 5. Electrical conductivity of PANI/DBSA as a function of PANI weight fraction at room temperature. The closed circles show *electronic* conductivity, as determined from linear current-voltage characteristics. At smaller weight fractions of PANI (such as 3.5 wt % or less), an *ionic* conduction becomes appreciable. The inset shows the imposed current profile used in the four-wire measurements.

lus is observed ($E' \sim \omega$). During the gelation process, E' becomes almost independent of frequency. The results of Figure 4 at 180 °C and below resemble those of the gelled structures in PVC/DOP.⁶ The 200 °C data qualitatively resemble the liquid-like, i.e., ungelled, behavior of PVC/DOP. Although the method used in this study does not fit well for actual rheological measurements in the fluid state, it is evident that an onset of a rheological transition is observed. The results also resemble the recent data on rheological order/disorder transitions of flexible polymer–amphiphile systems consisting of poly(4-vinylpyridine) hydrogen bonded to 3-pentadecylphenol which, due to noncorrosivity, allows detailed dynamic rheological investigations.⁴⁴

It can next be asked, whether the transition from an elastic gel to a viscous liquid (see Figure 3), due to decrease of PANI weight fraction, manifests also in the electrical conductivity. The room temperature conductivity of PANI/DBSA is shown in Figure 5 as a function of PANI weight fraction. The linear current–voltage-behavior indicates primarily *electronic* conductivity (Ohm's law) for PANI/DBSA containing more than ca. 7.3 wt % PANI. At lower weight fractions of PANI (such as 3.5 wt % or less), the current–voltage behavior is not purely Ohmic and a component of ionic conductivity is included, as is also suggested in the time dependence in the polarity reversal. At these low concentrations, the *electronic* conductivity of the network becomes less than the *ionic* conductivity of the DBSA background. Therefore, at room temperature, for the liquid-like samples of low PANI concentration, the ionic conductivity prevails suggesting that the chains are not in direct contact but are separated by ionically conducting DBSA medium. In contrast, for samples in the elastic gel state (>ca. 7 wt % PANI) an electronic conductivity is observed suggesting direct chain-to-chain hopping. This observation is in agreement with the networking concept.

The observed gel melting at elevated temperatures inspired us to study also the conductivity as a function of the temperature. The conductivities σ_T at the temperature T scaled by the room temperature conductivity $\sigma_{23^\circ\text{C}}$ for selected PANI/DBSA samples as a function of temperature are shown in Figure 6 for upward scans at the sweep rate of 5 °C/min. For the sample contain-

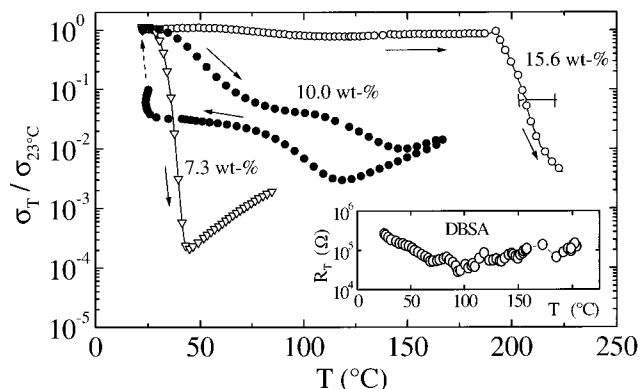


Figure 6. Conductivity at the temperature T scaled by room temperature conductivity of PANI/DBSA as a function of temperature at sweep rate 5 °C/min during heating. A triangular waveform of imposed current at the frequency of ca. 200 mHz has been used. For 10 wt %, the recovery after cooling has been qualitatively indicated.

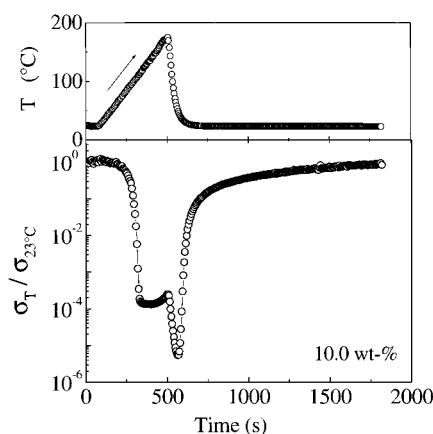


Figure 7. Conductivity at the temperature T scaled by room temperature conductivity of PANI/DBSA 10/90 (w/w) during rapid heating at 25 °C/min and immediate quenching back to room temperature within seconds.

ing 15.6 wt % PANI, a broad transition is observed between 190 and 225 °C where the conductivity drops ca. 3 orders of magnitude and approximately acquires the ionic conductivity level of DBSA. A very weak “secondary effect” is observed between 60 and 90 °C. For 10 wt %, two broad transitions are observed in the conductivity: between 35 and 70 °C and between 110 and 150 °C. For 7.3 wt % the transition is at ca. 30–40 °C. Note that in DBSA no such transitions are observed as shown in the inset of Figure 6. Minor dimensional changes of the samples during the measurements cannot explain these large changes in the conductivity. During cooling a strong hysteresis was observed, but eventually the original conductivity was restored, as indicated for the sample of 10 wt % in Figure 6. After the original conductivity had recovered, the conductivity behavior in repeated upward scans was similar to the first cycle shown. The conductivity transitions were observed at all studied heating rates ranging from 5 to 75 °C/min.

Figure 6 shows that there is a hysteresis in the conductivity during the temperature sweeps. However, the original room temperature conductivity was ultimately recovered. To assess the dynamics in more detail, the sample with 10.0 wt % PANI was studied more thoroughly, (see Figure 7). Heating at a relatively quick rate of 25 °C/min yields a rapid transition. Following a rapid quench to room temperature during

a few seconds, the conductivity relaxes slowly to the original value.

Discussion

In the previous section it was demonstrated that preparation of PANI/DBSA complexes in formic acid medium allows specific properties after removal of the formic acid:

(1) Fusible and homogeneous particle-free complexes are obtained at the resolution of optical microscopy. To appreciate this observation, the samples were also prepared differently. Firstly, dissolving PANI (EB) in DBSA directly without a third medium did not yield particle-free morphology, even when the mixing was performed at an elevated temperature of 200 °C. A probable explanation is that, due to its large size, DBSA cannot easily dissolve the *crystalline* regions of PANI. The previously observed mesomorphic order^{20,21} is, therefore, probably formed in the originally amorphous domains of PANI (EB). A processing medium therefore promotes dissolution. An ideal medium would be a common *small molecule* solvent of PANI (EB) and DBSA. However, there is an inherent difficulty in this respect: (i) Strong protonating acids are solvents for PANI, but they were ruled out because they could prevent the PANI complexation with DBSA. (ii) Basic solvents cause deprotonation. (iii) If the mixing of PANI and DBSA was performed in nonacidic (i.e., nonsolvent) medium, such as ethanol, undissolved particles remained in the final PANI/DBSA film. Therefore, we tried to find an sufficiently *acidic* processing medium where the crystalline domains of PANI are at least swollen but would not compete with DBSA in protonation. This consideration suggested formic acid, because it is a solvent for oligomeric PANI but could only swell polymeric PANI.

(2) At low temperatures (i.e., at $T < T_{\text{gel}}$) and for intermediate weight fractions (i.e., ca. 7–15 wt % PANI), the gel state is encountered showing elastic behavior, essentially frequency independent storage modulus, and electrical conductivity of an *electronic* nature. Such behavior agrees with a structure where the comb-shaped PANI(DBSA)_{1,0} chains form interconnected networks in the DBSA background. At lower PANI concentrations, viscous fluids with less elastic behavior are observed, whereas for higher concentrations infusible material is observed. When a gel is heated above T_{gel} the conductivity drops to the value corresponding to the *ionic* conductivity of DBSA. This observation agrees with a hypothesis that the *electrically percolating* network structure formed by PANI(DBSA)_{1,0} is at least partly dissolved. There the material flows without elastic response and shows frequency dependent moduli which are typical for viscous fluids.

Qualitatively, the gelation and melting have here been demonstrated using several methods. *Quantitatively*, one observes ungratifying scatter in the melting point data (see Figure 3). Two possible reasons are given: (i) The amount of residual water may vary from sample to sample, in spite of prolonged drying. (ii) To obtain fully reproducible results in the case of the “classical gels” with relatively low T_{gel} , the samples are usually stored for extensively long time periods at $T > T_{\text{gel}}$ to guarantee complete dissolution and, subsequently, at $T < T_{\text{gel}}$ to achieve homogeneity in the gel formation. In our case with T_{gel} nearly 200 °C, long homogenization periods at high temperatures could not be used.

One can also compare the gel melting temperatures for PANI/DBSA 10/90 (w/w) obtained using different

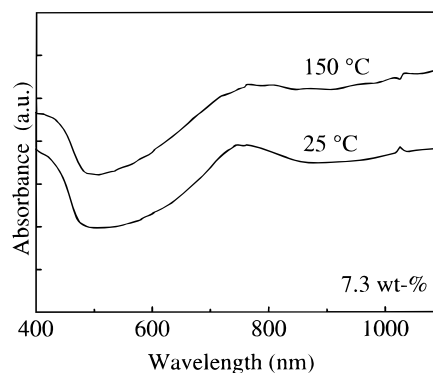


Figure 8. UV/vis absorption spectra of PANI/DBSA with 7.3 wt % at 25 °C (i.e., $< T_{\text{gel}}$) and at 150 °C (i.e., $> T_{\text{gel}}$).

methods. The dynamic moduli as a function of frequency suggest gel melting between 180 and 200 °C in the isothermal measurements. The modified BDM method rendered $T_{\text{gel}} = 180$ °C using the heating rate 3 °C/min. A weak “secondary transition” is observed between 30 and 80 °C (see inset of Figure 3). Two transitions are observed also in the conductivity measurements at 5 °C/min: It is tempting to assign the upper transition between 110 and 150 °C with the gel melting. A “secondary transition” between 35 and 70 °C is observed, as also manifested in Figure 3. The reason for this transition is not known to us presently. Therefore, although quantitative agreement hardly can be claimed, widely different methods with different “histories” render results that are not very far from each other, especially taking into account the error bars in the temperatures.

Next we turn to various arguments that probe the validity of the above model, i.e., the nature of the gel state and the physical cross-links, effect of absorbed water, and possible dedoping effects.

Figure 8 illustrates UV/vis data for the sample containing 7.3 wt % PANI. Similar polaronic peaks at 780 nm are observed at both 25 and 150 °C, i.e., below and above the conduction transition shown in Figure 6, suggesting that the conductivity transition is not due to dedoping effects. In other words, the DBSA molecules that are bonded to the *iminic* nitrogen of PANI, due to charge transfer due to doping, remain bonded even in the liquid state. Such conclusion is also suggested using poly(vinylpyridine) complexes with sulfonic acids which allow high resolution FTIR studies as a function of temperature.⁴⁵ Therefore, we suggest that the conductivity transition is due to morphological changes.

Polymers that have flexible backbones but are stiffened by covalently bound long alkyl chains to form comb-shaped polymers, such as poly(alkyl acrylates), are known to undergo gelation in suitable solvents such as alkyl alcohols and hydrocarbons.⁷ In this case a necessary condition has been shown to be that the side chains are long enough, typically more than 12 methyl units in which case the physical cross-links are formed due to the side chain crystallization. WAXS data for PANI/DBSA shows no essential crystallinity (see Figure 9), probably due to the relatively short and branched alkyl chains. Therefore, the mechanism to form physical cross-links is not expected to be the side chain crystallization as in poly(alkyl acrylate)/alkyl alcohol, for example.

The structures were further studied using SAXS. As a background, it is first helpful to study self-organization in DBSA/water systems. Figure 10a shows that pure DBSA does not show a SAXS peak, i.e., it is not

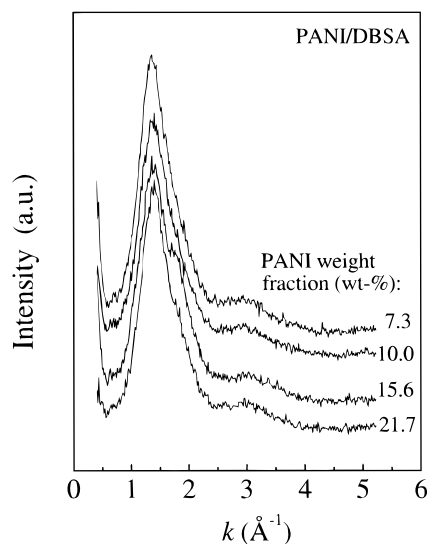


Figure 9. WAXS data for PANI/DBSA with different PANI weight fractions.

mesomorphic. Instead, a broad and shallow peak is observed at 0.328 \AA^{-1} (corresponding to 19.2 \AA) probably due to correlation effects. FTIR measurements show the characteristic absorption of the sulfonic acid group— SO_3H at 906 cm^{-1} . For DBSA/ H_2O 75/25 (w/w), a distinct and narrow SAXS peak is observed at 0.209 \AA^{-1} and even the second order peak at 0.414 \AA^{-1} is observable, indicating smectic order at long period of 30 \AA . FTIR shows that samples with added water show reduced absorption at 906 cm^{-1} and increased absorption at the sulfonate band at ca. 1200 cm^{-1} . Therefore, sulfonic acid groups protonate the water molecules to form $(\text{SO}_3^-)(\text{H}_3\text{O}^+)$. Thus, the increased polar/nonpolar repulsion favors formation of mesomorphic structures in DBSA/water systems due to added water.

Figure 10b shows the SAXS intensity curves for the sample containing 15.6 wt % PANI in DBSA at two temperatures, first measured at $220 \text{ }^\circ\text{C}$ and then at $20 \text{ }^\circ\text{C}$ immediately after cooling. The particular sample did not totally soften even at the higher temperature. Note that this high PANI concentration renders samples that are near the limit of processibility where in some samples (such as the present one) only partial but not complete gel melting was obtained below ca. $220 \text{ }^\circ\text{C}$ which we regarded as the maximum allowable measurement temperature (see Figure 3). At both temperatures broad SAXS peaks with relatively small intensity are observed at $k = 0.236 \text{ \AA}^{-1}$ (corresponding to long periods of ca. 26.6 \AA) without clear indication of the second-order peaks. At least two options exist for the interpretation. The peaks may be due to either mesomorphic structure with a relatively poor order or concentration fluctuations (for closely related systems, see refs 46 and 47). At present, the first alternative would offer a more natural explanation for the observed gel behavior where the physical cross-link sites would then be localized mesomorphic domains formed by $\text{PANI}(\text{DBSA})_{1.0}$ with the long period 26.6 \AA . The rest of the material would be disordered $\text{PANI}(\text{DBSA})_{1.0}$ swollen by additional DBSA. Figure 10c shows the case for PANI/DBSA for 7.3 wt % PANI measured first at $190 \text{ }^\circ\text{C}$ and then at $20 \text{ }^\circ\text{C}$ immediately after cooling to room temperature. At $190 \text{ }^\circ\text{C}$ hardly any peak is observed, whereas cooling to $20 \text{ }^\circ\text{C}$ renders a larger but broad peak at 0.246 \AA^{-1} (corresponding to 25.6 \AA). The transition is gradual. An interpretation is suggested where localized mesomorphic structures are observed

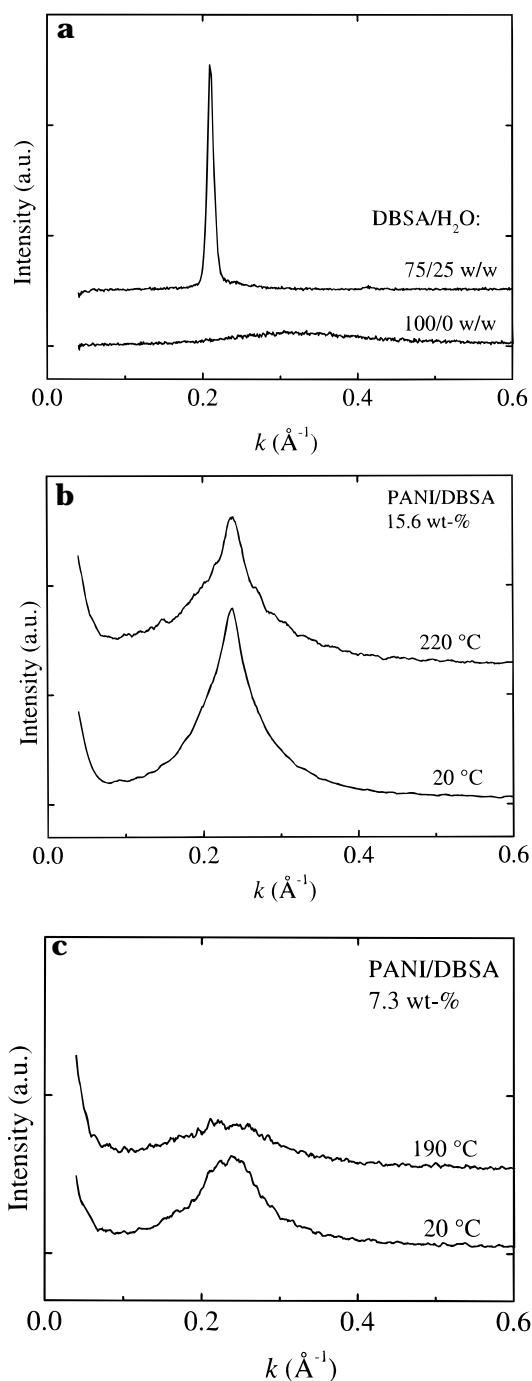


Figure 10. SAXS data for (a) isotropic pristine DBSA and smectic mixture consisting of 75 wt % DBSA and 25 wt % H_2O , (b) PANI/DBSA with 15.6 wt % PANI at 220 and $20 \text{ }^\circ\text{C}$, and (c) PANI/DBSA with 7.3 wt % PANI at 190 and $20 \text{ }^\circ\text{C}$.

at $20 \text{ }^\circ\text{C}$ which also act as the physical cross-links that manifest in the mechanical measurements. Heating to $190 \text{ }^\circ\text{C}$ yields fluid-like behavior with only correlation effects.

Note that one has to be particularly careful with the interpretations of SAXS results due to potentially absorbed water. Some samples were intentionally exposed to atmospheric humidity. Consequently, another distinct SAXS peak was observed at 0.191 \AA^{-1} in addition to the above peak at 0.236 \AA^{-1} in Figure 10b, indicating that the DBSA/water system forms another level of self-organization and the peaks shown are not due to self-organization of DBSA with possible residual water within PANI/DBSA.

Effect of potentially absorbed or residual water can be discussed on the basis of rigid rod polymers. Spinning of ultra-high-strength fibers of PBT consists of an initial dissolution of the polymer in strong acids such as dry MSA. Washing with a coagulant, which is a nonsolvent such as water, results in fibrous structures. The fibrillar structure in such and related systems depends on how the nonsolvent is introduced, the extreme being just the penetration of the atmospheric humidity.^{9,10,48} Complicated phase behavior is observed.^{49,50}

Therefore, it is feasible to discuss the present PANI gels in the context of a polymer-solvent-nonsolvent framework. Let us first discuss the possibility of residual formic acid. Formic acid can be strongly bound to certain polymers, for example, to the ones containing imidazole groups to form crystallo-solvates.⁵¹ For these systems, only heat treatment at about 200 °C is able to remove all of the formic acid. In the present case, the samples were first dried for 1 week in vacuum at 60 °C and subsequently heated to 200 °C. Therefore, we expect that there is very little, if any, formic acid left, which is also indicated by mass spectrometry and FTIR showing no signs of residual formic acid.

It seems, that residual or absorbed water may have more profound effects in our case. Sulfonic acids are strongly hygroscopic because the acid group is able to dissociate and hydrogen bond. Therefore, it is very difficult to achieve totally anhydrous sulfonic acids.⁴² Even more, residual water may also be bound to PANI. Based on the previous literature dealing with hydrogen-bonding polymers, such as poly(bisbenzimidazobenzophenanthrolinedione),⁴⁸ it may be expected that a complete removal of water would require prolonged drying at elevated temperatures (such as at 200 °C for several days in vacuum⁴⁸) that are susceptible to yield chemical cross-linking of PANI. In addition, formic acid also seems to slightly decompose to produce water. Therefore, it is possible that traces of water are present in our samples, below the resolution of our SAXS. Note that the previous literature concerning PBLG/DMF suggests that water content of even less than 1% is able to cause emergence of "complicated phases", i.e., aggregates.¹¹

Concluding Remarks

We have shown that polyaniline in dodecylbenzene-sulfonic acid (DBSA) solvent is able to form thermoreversible, i.e., fusible, gels which show behavior close to ideal rubber elasticity in the gel state for $T < T_{\text{gel}}$ and liquid behavior for $T > T_{\text{gel}}$. An essential observation is that, in order to achieve sufficiently homogeneous complexation between PANI and DBSA, the complexes have to be prepared in formic acid that is completely removed at the end. Formic acid does not compete with DBSA in protonation but is able to swell the crystalline domains of PANI to promote its dissolution in DBSA. Network structures, i.e., gels, for $T < T_{\text{gel}}$ manifest as the elastic behavior in compression tests, roughly frequency independent storage moduli, and electrical conductivity which is Ohmic. Thus the percolative network is suggested based on both viscoelastic and conductivity arguments. The SAXS results preliminarily suggest that the physical cross-links are due to localized mesomorphic domains within the disordered background. This kind of cross-linking allows facile fusibility, unlike the previously reported PANI gels where the crystalline cross-links can be purged only

with difficulty, if at all. At elevated temperatures $T > T_{\text{gel}}$ or at low weight fraction of PANI, a viscous fluid state is obtained, characteristic of frequency dependent moduli and conductivity of DBSA medium, explained as at least partly dissolved PANI chains.

Thermoreversible gels based on electrically conductive polymers interestingly combine the effects of networking with the electrical and mechanical behavior and thus offer a novel class of processible materials. They may also explain the attractive conductivity properties under tension in other PANI-surfactant complexes blended with thermoplastic elastomers.^{52,53}

Acknowledgment. We are grateful to Jan-Erik Österholm, Yong Cao, Gerrit ten Brinke, Kalle Levon, and Heidi Österholm for discussions on various aspects related to polymer surfactant complexation. We acknowledge Juha Tanner and Tapio Mäkelä for experimental assistance and discussions, Kim Wickström of Neste Oy (Finland) for mass spectrometry measurements, and Milja Karjalainen of Helsinki University for WAXS measurements. Neste Chemicals is acknowledged for permission to publish the results. Jukka Seppälä is acknowledged for permission to use FTIR and UV/vis instruments of his laboratory. This work has been supported by Neste Chemicals, the Technology Development Centre (Finland), and the Neste Foundation.

References and Notes

- (1) *Physical Networks; Polymers and Gels*; Burchard, W., Ross-Murphy, S. B., Eds.; Elsevier: London, 1990.
- (2) Hiltner, A.; Baer, E. *Polym. Prepr. (Am. Chem. Soc., Div. Polym. Chem.)* **1986**, 27, 207.
- (3) *Reversible Polymeric Gels and Related Systems*; Russo, P. S., Ed.; American Chemical Society: Washington, DC, 1987; Vol. 350.
- (4) Guenet, J.-M. *Trends Polym. Sci.* **1995**, 4, 6.
- (5) Guenet, J.-M. *Thermoreversible Gelation of Polymers and Biopolymers*; Academic Press: London, 1992.
- (6) te Nijenhuis, K. In *Physical Networks; Polymers and Gels*; Burchard, W., Ross-Murphy, S. B., Eds.; Elsevier: London, 1990.
- (7) Platé, N. A.; Shibaev, V. P. *Comb-Shaped Polymers and Liquid Crystals*; Plenum Press: New York and London, 1987.
- (8) Allen, S. R.; Filippov, A. G.; Farris, R. J.; Thomas, E. L.; Wong, C.-P.; Berry, G. C.; Cheveney, E. C. *Macromolecules* **1981**, 14, 1135.
- (9) Cohen, Y.; Frost, H. H.; Thomas, E. L. In *Reversible Polymeric Gels and Related Systems*; Russo, P. S., Ed.; American Chemical Society: Washington, DC, 1987; Vol. 350.
- (10) Se, K.; Berry, G. C. In *Reversible Polymeric Gels and Related Systems*; Russo, P. S., Ed.; American Chemical Society: Washington, DC, 1987; Vol. 350.
- (11) Russo, P. S.; Miller, W. G. *Macromolecules* **1984**, 17, 1324.
- (12) Cohen, Y.; Dacan, A. *Macromolecules* **1995**, 28, 7638.
- (13) *High Performance Polymers and Composites*; Kroschwitz, J. I., Ed.; Wiley: New York, 1991.
- (14) Geniès, E. M.; Boyle, A.; Lapkowski, M.; Tsintavis, C. *Synth. Met.* **1990**, 36, 139.
- (15) MacDiarmid, A. G.; Epstein, A. J. *Mater. Res. Soc. Symp. Proc.* **1994**, 328, 133.
- (16) Chiang, J.-C.; MacDiarmid, A. G. *Synth. Met.* **1986**, 13, 193.
- (17) Doriomedoff, M.; Hautiere-Cristofini, F.; Surville, R. D.; Jozefowicz, M.; Yu, L.-T.; Buvet, R. *J. Chim. Phys. Physicochim. Biol.* **1971**, 68, 1055.
- (18) Andreatta, A.; Cao, Y.; Chiang, J. C.; Heeger, A. J.; Smith, P. *Synth. Met.* **1988**, 26, 383.
- (19) Cao, Y.; Smith, P.; Heeger, A. J. *Synth. Met.* **1992**, 48, 91.
- (20) Zheng, W.-Y.; Wang, R.-H.; Levon, K.; Rong, Z. Y.; Taka, T.; Pan, W. *Makromol. Chem. Phys.* **1995**, 196, 2443.
- (21) Levon, K.; Ho, K.-H.; Zheng, W.-Y.; Laakso, J.; Kärnä, T.; Taka, T.; Österholm, J.-E. *Polymer* **1995**, 36, 2733-8.
- (22) Ikkala, O. T.; Pietilä, L.-O.; Ahjopalo, L.; Österholm, H.; Passiniemi, P. J. *J. Chem. Phys.* **1995**, 103, 9855.
- (23) Kärnä, T.; Laakso, J.; Niemi, T.; Ruohonen, H.; Savolainen, E.; Lindström, H.; Virtanen, E.; Ikkala, O.; Andreatta, A. U.S. Patent No. 5,340,499, 1994.

- (24) Ikkala, O.; Passiniemi, P. J. U.S. Patent No. 5,520,852, 1996.
- (25) Vikki, T.; Pietilä, L.-O.; Österholm, H.; Ahjopalo, L.; Takala, A.; Toivo, A.; Levon, K.; Passiniemi, P.; Ikkala, O. *Macromolecules* **1996**, *29*, 2945.
- (26) MacDiarmid, A. G.; Min, Y.; Wiesinger, J. M.; Oh, E. J.; Scherr, E. M.; Epstein, A. J. *Synth. Met.* **1993**, *55–57*, 753.
- (27) Tzou, K.; Gregory, R. V. *Synth. Met.* **1993**, *55–57*, 983.
- (28) Gettinger, C. L.; Heeger, A. J.; Pine, D. J.; Cao, Y. *Synth. Met.* **1995**, *74*, 81.
- (29) Angelopoulos, M.; Liao, Y.-H.; Furman, B.; Graham, T. *Macromolecules* **1996**, *29*, 3046.
- (30) Tzou, K.; Gregory, R. V. *Synth. Met.* **1995**, *69*, 109.
- (31) Yoshino, K.; Nakao, K.; Onoda, M.; Sugimoto, R.-I. *Solid State Commun.* **1989**, *70*, 609.
- (32) Yoshino, K.; Nakao, K.; Onoda, M. *J. Phys.: Condens. Matter* **1990**, *2*, 2857.
- (33) Morita, S.; Kawai, T.; Yoshino, K. *J. Appl. Phys.* **1991**, *69*, 4445.
- (34) Yang, C. Y.; Cao, Y.; Smith, P.; Heeger, A. J. *Synth. Met.* **1993**, *53*, 293.
- (35) Wang, Y.; Rubner, M. F. *Macromolecules* **1992**, *25*, 3284.
- (36) Adriaanse, L. J.; Reedijk, J. A.; Teunissen, P. A. A.; Brom, H. B.; Michels, M. A. J.; Brokken-Zijp, J. C. M. *Phys. Rev. Lett.* **1997**, *78*, 1755.
- (37) Wessling, B. *Adv. Mater.* **1993**, *5*, 300.
- (38) Banerjee, P.; Mandal, B. M. *Macromolecules* **1995**, *28*, 3940.
- (39) Stejskal, J.; Kratochvil, P.; Armes, S. P.; Lascelles, S. F.; Riede, A.; Helmstedt, M.; Prokes, J.; Krivka, I. *Macromolecules* **1996**, *29*, 6814.
- (40) Cohen Addad, J. P. *Physical Properties of Polymeric Gels*; John Wiley & Sons: New York, 1996.
- (41) Cao, Y.; Andreatta, A.; Heeger, A. J.; Smith, P. *Polymer* **1989**, *30*, 2305.
- (42) Vold, M. J. *J. Am. Chem. Soc.* **1941**, *63*, 1427.
- (43) Takahashi, A.; Sakai, M.; Kato, T. *Polym. J. (Tokyo)* **1980**, *12*, 335.
- (44) Ruokolainen, J.; Torkkeli, M.; Serimaa, R.; Komanschek, B. E.; ten Brinke, G.; Ikkala, O. *Macromolecules* **1997**, *30*, 2002.
- (45) Ruokolainen, J.; ten Brinke, G.; Ikkala, O. et al. To be published.
- (46) Huh, J.; Ikkala, O.; ten Brinke, G. *Macromolecules* **1997**, *30*, 1828.
- (47) Ruokolainen, J.; Torkkeli, M.; Serimaa, R.; Komanschek, E.; Ikkala, O.; ten Brinke, G. *Phys. Rev. E* **1996**, *54*, 6646.
- (48) Wong, C.-P.; Berry, G. C. *Polymer* **1979**, *20*, 229.
- (49) Cohen, Y.; Cohen, E. *Macromolecules* **1995**, *28*, 3631.
- (50) Cohen, Y.; Saruyama, Y.; Thomas, E. L. *Macromolecules* **1991**, *24*, 1161.
- (51) Ginzburg, B. M.; Mikhailova, N. V.; Nikitin, V. N.; Sidorovich, A. V.; Tuichiev, Sh.; Frenkel, S. Yu. *Polym. Sci. USSR* **1967**, *9*, 2694.
- (52) Ikkala, O.; Kirmanen, P.; Savolainen, E.; Virtanen, E. International PCT Patent Application WO 95/22151, 1994.
- (53) Ikkala, O. T.; Laakso, J.; Väkiparta, K.; Virtanen, E.; Ruohonen, H.; Järvinen, H.; Taka, T.; Passiniemi, P.; Österholm, J.-E.; Cao, Y.; Andreatta, A.; Smith, P.; Heeger, A. J. *Synth. Met.* **1995**, *69*, 97.

MA9615056